Lauterborn *et al.*, *Neuroscience* **68**, 363 (1995).
22. F. Zafra, E. Castrén, H. Thoenen, D. Lindholm, *Proc. Natl. Acad. Sci. U.S.A.* **88**, 10037 (1991); F. Zafra, D. Lindholm, E. Castrén, J. Hartikka, H. Thoenen, *J. Neurosci.* **12**, 4793 (1992); M. P. Berzaghi *et al.*, *ibid.* **13**, 3818 (1993).
23. B. Berninger *et al.*, *Development* **121**, 2327 (1995).
24. P. Emfors *et al.*, *Neuron* **7**, 165 (1991); P. J. Isackson *et al.*, *ibid.* **6**, 937 (1991); M. M. Dugich-Djordjevic *et al.*, *Neuroscience* **47**, 303 (1992).
25. E. Castrén, F. Zafra, H. Thoenen, D. Lindholm, *Proc. Natl. Acad. Sci. U.S.A.* **89**, 9444 (1992).
26. Y. Fregnac and M. Imbert, *J. Physiol. (London)* **278**, 27 (1978).
27. E. Castrén *et al.*, *Neuroscience* **64**, 71 (1995).
28. LTP is the paradigm most widely used to characterize cellular and molecular events underlying neuronal plasticity and is also thought to be representative for processes involved in learning and memory [see T. V. Bliss and G. L. Collingridge, *Nature* **361**, 31 (1993)]. The field excitatory postsynaptic potentials recorded in the dentate gyrus are augmented for hours after a conditioning tetanic stimulus. The same stimulation parameters that lead to LTP in this system resulted in a marked increase in BDNF mRNA and a smaller increase in NGF mRNA, but no increase in NT-3 and NT-4/5 mRNAs in the dentate gyrus [E. Castrén *et al.*, *Neuroreport* **4**, 895 (1993); M. Dragunow *et al.*, *Neurosci. Lett.* **160**, 232 (1993)]. Similar observations were also made in hippocampal slice preparations [S. L. Patterson, L. M. Grover, P. A. Schwartzkroin, M. Bothwell, *Neuron* **9**, 1081 (1992)], in which the stimulation of the Schaffer collaterals (originating from CA3 and projecting to CA1 hippocampal neurons) induced a marked increase in BDNF mRNA and a slight increase in NT-3 mRNA in the CA1 region. Even the rearing of rats in an "enriched environment," leading to an improvement in spatial memory, was associated with an increase in hippocampal BDNF mRNA [T. Falkenberg *et al.*, *Neurosci. Lett.* **138**, 153 (1992)].
29. C. E. Bandtlow *et al.*, *EMBO J.* **6**, 891 (1987).
30. D. L. Shelton and L. F. Reichardt, *J. Cell Biol.* **102**, 1940 (1986); H. Rohrer, R. Heumann, H. Thoenen, *Dev. Biol.* **128**, 240 (1988).
31. E.-M. Barth, S. Korsching, H. Thoenen, *J. Cell Biol.* **99**, 839 (1984).
32. O. Griesbeck, A. Blöchl, J. F. Carnahan, H. Nawa, H. Thoenen, *Soc. Neurosci. Abstr.* **21** (part 2), 1046 (1995).
33. P. DeCamilli and R. Jahn, *Annu. Rev. Physiol.* **52**, 625 (1990); A. Thureson-Klein and R. L. Klein, *Int. Rev. Cytol.* **121**, 67 (1990); M. Matteoli and P. DeCamilli, *Curr. Opin. Neurobiol.* **1**, 91 (1991).
34. Neuronal acetylcholinesterase, like NGF and BDNF, is secreted in an activity-dependent manner by neurons, including dendrites [S. A. Greenfield, *Neurochem. Int.* **7**, 887 (1985); J. Weston and S. A. Greenfield, *Neuroscience* **17**, 1079 (1986); M. E. Appleyard, J. L. Vercher, S. A. Greenfield, *ibid.* **25**, 133 (1988)]. Unlike NTs, its release depends on extracellular calcium and cannot be blocked by tetrodotoxin (*14*).
35. W. Huttner, unpublished data.
36. A. Blöchl and H. Thoenen, unpublished data.
37. T. C. Südhof, P. de Camilli, H. Niemann, R. Jahn, *Cell* **75**, 1 (1993).
38. J. H. Williams *et al.*, *Nature* **341**, 739 (1989); M. Zhuo *et al.*, *Science* **260**, 1946 (1993); D. M. Bannerman *et al.*, *J. Neurosci.* **14**, 7415 (1994); M. K. Meffert *et al.*, *Neuron* **13**, 1225 (1994); K. P. S. J. Murphy *et al.*, *Neuropharmacology* **33**, 1375 (1994); E. M. Schuman and D. V. Madison, *Science* **263**, 532 (1994); *Annu. Rev. Neurosci.* **17**, 153 (1994).
39. M. P. Berzaghi, R. Gutiérrez, U. Heinemann, D. Lindholm, H. Thoenen, *Soc. Neurosci. Abstr.* **21** (part 1), 545, (1995).
40. B. Knüsel and F. Hefti, *J. Neurochem.* **59**, 1987 (1992).
41. B. Berninger, D. E. Garcia, N. Inagaki, C. Hahnel, D. Lindholm, *Neuroreport* **4**, 1303 (1993).
42. B. Berninger and H. Thoenen, unpublished data.
43. M. Korte *et al.*, *Proc. Natl. Acad. Sci. U.S.A.* **92**, 8856 (1995).
44. M. Korte, O. Griesbeck, H. Thoenen, T. Bonhoeffer, unpublished data.
45. L. Maffei *et al.*, *J. Neurosci.* **12**, 4651 (1992).
46. G. Carmignoto *et al.*, *J. Physiol. (London)* **464**, 343 (1993); A. Fiorentini *et al.*, *Vis. Neurosci.* **12**, 51 (1995).
47. R. J. Cabelli *et al.*, Science **267**, 1662 (1995).
48. R. A. W. Galuske, D. S. Kim, E. Castrén, W. Singer, *Soc. Neurosci. Abstr.* **20** (part 1), 312 (1994).
49. T. N. Wiesel and D. H. Hubel, *J. Neurophysiol.* **26**, 1003 (1963); D. H. Hubel and T. N. Wiesel, *J. Physiol. (London)* **206**, 419 (1970); S. LeVay, T. N. Wiesel, D. H. Hubel, *J. Comp. Neurol.* **179**, 223 (1980).
50. M. F. Bear, A. Kleinschmidt, Q. Gu, W. Singer, *J. Neurosci.* **10**, 909 (1990).
51. T. Kasamatsu and J. D. Pettigrew, *Science* **194**, 206 (1976); M. F. Bear and W. Singer, *Nature* **320**, 172 (1986); Q. Gu and W. Singer, *Eur. J. Neurosci.* **7**, 1146 (1995).
52. L. Domenici *et al.*, *Proc. Natl. Acad. Sci. U.S.A.* **88**, 8811 (1991).
53. C. J. Shatz, *Neuron* **5**, 745 (1990).
54. N. Berardi *et al.*, *Proc. Natl. Acad. Sci. U.S.A.* **91**, 684 (1994); L. Domenici, A. Cellerino, N. Berardi, A. Lattaneo, L. Maffei, *Neuroreport* **5**, 2041 (1994).
55. S. B. McMahon, D. L. H. Bennett, J. V. Priestley and D. L. Shelton [*Nature Med.* **1**, 774 (1995)] have demonstrated that a fusion protein made from the extracellular domain of TrkA and the constant portion of human IgG blocked the effects of exogenous NGF in vitro and of endogenous NGF in vivo. An analogous construct made from the extracellular domain of TrkB and the constant portion of human IgG has been used for local infusion to the visual cortex of kittens during the critical period, where it prevented, in preliminary experiments, the formation of ocular dominance columns (R. J. Cabelli and C. J. Shatz, unpublished data), as did the local infusion of BDNF and NT-4/5 (*47*).
56. L. Domenici, G. Fontanesi, A. Cattaneo, P. Bagnoli, L. Maffei, *Vis. Neurosci.* **11**, 1093 (1995).
57. D. M. Holtzman *et al.*, *J. Neurosci.* **15**, 1567 (1995).
58. K. Stoeckel, M. Dumas, H. Thoenen, *Neurosci. Lett.* **10**, 61 (1978).
59. H. O. Reiter and M. P. Stryker, *Proc. Natl. Acad. Sci. U.S.A.* **85**, 3623 (1988).
60. M. Mayford, T. Abel, E. R. Kandel, *Curr. Opin. Neurobiol.* **5**, 141 (1995).
61. T. Timmusk *et al.*, *Neuron* **10**, 475 (1993).
62. H. Misawa, K. Ishii, T. Deguchi, *J. Biol. Chem.* **267**, 20392 (1992); P. Lönnerberg *et al.*, *Proc. Natl. Acad. Sci. U.S.A.* **92**, 4046 (1995).
63. K. F. Kozarsky and J. M. Wilson, *Curr. Opin. Genet. Dev.* **3**, 499 (1993).
64. W. Singer *et al.*, *Brain Res.* **134**, 568 (1977).
65. I thank A. Blöchl and B. Berninger for providing unpublished data; Y.-A. Barde, T. Bonhoeffer, A. Cellerino, M. Korte, D. Lindholm, and W. Singer for critically reading the manuscript; J. Cooper for linguistic revision; I. Hajjar and E. Hering for secretarial help; and C. Bauereiss and J. Chalcroft for artwork.

RESEARCH ARTICLE

Biostratigraphic and Geochronologic Constraints on Early Animal Evolution

John P. Grotzinger, Samuel A. Bowring, Beverly Z. Saylor, Alan J. Kaufman

Two distinct evolutionary pulses, represented by the Vendian Ediacaran fauna and Cambrian small shelly faunas, are generally thought to characterize the emergence of macroscopic animals at the end of Precambrian time. Biostratigraphic and uranium-lead zircon age data from Namibia indicate that most globally distributed Ediacaran fossils are no older than 549 million years old and some are as young as 543 million years old, essentially coincident with the Precambrian-Cambrian boundary. These data suggest that the most diverse assemblages of Ediacaran animals existed within 6 million years of the Precambrian-Cambrian boundary and that simple discoid animals may have appeared at least 50 million years earlier.

Early animal evolution is widely thought to have occurred in two discrete steps, set apart by tens of millions of years. Evolutionary models have had to explain an initial episode at the end of Precambrian time (Vendian Period) in which simple, mostly soft-bodied, cnidarian-grade organisms, bilaterians, and problematica (collectively referred to as the Ediacaran fauna) first appeared, followed by a second phase early in the Cambrian Period in which small shelly invertebrates (*1*) and complex trace fossils appeared in the Nemakit-Daldyn stage and rapidly diversified during the subsequent Tommotian, Adtabanian, and Botomian stages (*2–8*). Because the affinities of the earlier, Ediacaran fauna are still debated (compare *5*, *9*, *10*), the apparent wide separation in time of these two evolutionary pulses has been used to support phylogenetic arguments that these creatures are not simple precursors to later forms, but instead

J. P. Grotzinger, S. A. Bowring, and B. Z. Saylor are in the Department of Earth, Atmospheric and Planetary Sciences, Massachusetts Institute of Technology, Cambridge, MA 02139 USA. A. J. Kaufman is in the Department of Earth and Planetary Sciences Harvard University, Cambridge, MA 02138 USA.

represent a failed lineage, perhaps unrelated to the animal kingdom (*4–7, 11, 12*).

Temporal calibration of past evolutionary events, correlated using emerging biostratigraphic, chemostratigraphic, and magnetostratigraphic data sets, is possible only with precise absolute age control such as that offered by U-Pb zircon dating of volcanic rocks intercalated within sedimentary successions (*13–15*). In this article, we report new biostratigraphic and U-Pb radiometric age data from sedimentary and volcanic rocks of the Vendian-Cambrian Nama Group in southern Namibia. Biostratigraphic constraints are provided by specimens of the common Ediacaran taxon *Pteridinium* and a second frond-like form of uncertain affinity, complex spiral burrows of possibly late Vendian age, the Early Cambrian trace fossils *Phycodes pedum*, *P. coronatum*, and *Curvolithus*, and a new form of skeletalized fossil whose stratigraphic range is similar to that of *Cloudina*. Volcanic rocks were selected for dating that give the maximum age of the youngest Ediacaran fossils, the minimum duration of the Ediacaran fauna, the minimum age of the oldest skeletalized fossils, and the age of the Precambrian-Cambrian boundary. The dated sections have excellent chemostratigraphic tie points and fossil assemblages.

The Vendian time scale. For the Phanerozoic Eon, the geologic time scale primarily is based on a chronostratigraphy of biological events that are calibrated in absolute time with radiometric age determinations. The biostratigraphic basis for the Vendian time scale has been slow in developing. With the exception of simple, disk-shaped impressions of possible soft-bodied metazoans that occur in strata immediately below a Varanger-aged (*16*) glacial unit in the Mackenzie Mountains, Canada (*17*), all other occurrences of soft-bodied impressions are in strata younger than the Varanger glacial rocks (*18*). These younger impressions constitute the Ediacaran fauna, which was long thought to have been restricted to the first half of Vendian time. The apparent absence of Ediacaran fossils in younger Vendian strata provided the basis for erecting the Kotlin interval of the Vendian System (*16, 19, 20*). It has not been possible to recognize distinct biozones within Ediacaran-bearing strata because of taphonomic, paleoenvironmental, and possibly biogeographical factors (*3*), although recently it has been argued that some broad trends are apparent in their diversity (*21, 22*). Acritarchs may be useful in slightly older and younger rocks, but cannot be used to subdivide Ediacaran fossil ranges (*20*). Trace fossils and shelly fossils provide additional help but have low diversities throughout the Vendian (*23, 24*).

The carbon isotope record is proving to be critically important in unravelling Vendian history. As more and more sections are evaluated, it has become clear that the Vendian can be subdivided based on the oscillatory pattern of carbon isotope ratios (*18, 25*). As currently understood, the Vendian carbon isotope curve, beginning with the first rocks deposited above the Varanger glacial unit, features a shift to progressively lighter values and reaches a minimum ($\delta^{13}C_{carb}$ = −2 to −4 per mil relative to the PDB standard). It then increases to a maximum of about +4 to +5 per mil before decreasing to values that remain near 0 to +2 per mil until the close of Proterozoic time, when values decrease abruptly to −2 to −3 per mil just below the Precambrian-Cambrian boundary (*18, 21, 25, 26*). These excursions provide an independent framework against which to compare the temporal distribution of Ediacaran, trace fossil, and skeletal faunas.

Age estimates for the Vendian time scale and Precambrian-Cambrian boundary. Reliable age estimates for the Vendian time scale are sparse. Volcanic and intrusive rocks that underlie Varanger-age glaciogenic rocks are dated at 602 ± 3 Ma (million years ago) in Massachusetts (*27*) and 606 ± 3.7/− 2.9 in Newfoundland (*28*). We accept 600 Ma as the best maximum estimate for the age of the Varanger glacial event.

A volcanic ash bed interbedded with Ediacaran fossils in the Mistaken Point Formation of Newfoundland provides a direct U-Pb zircon age of 565 ± 3 Ma (*29*). Volcanic rocks of the Slawatycze Formation in Poland have a U-Pb zircon age of 551 ± 4 Ma (*30*), but provide only an indirect esti-

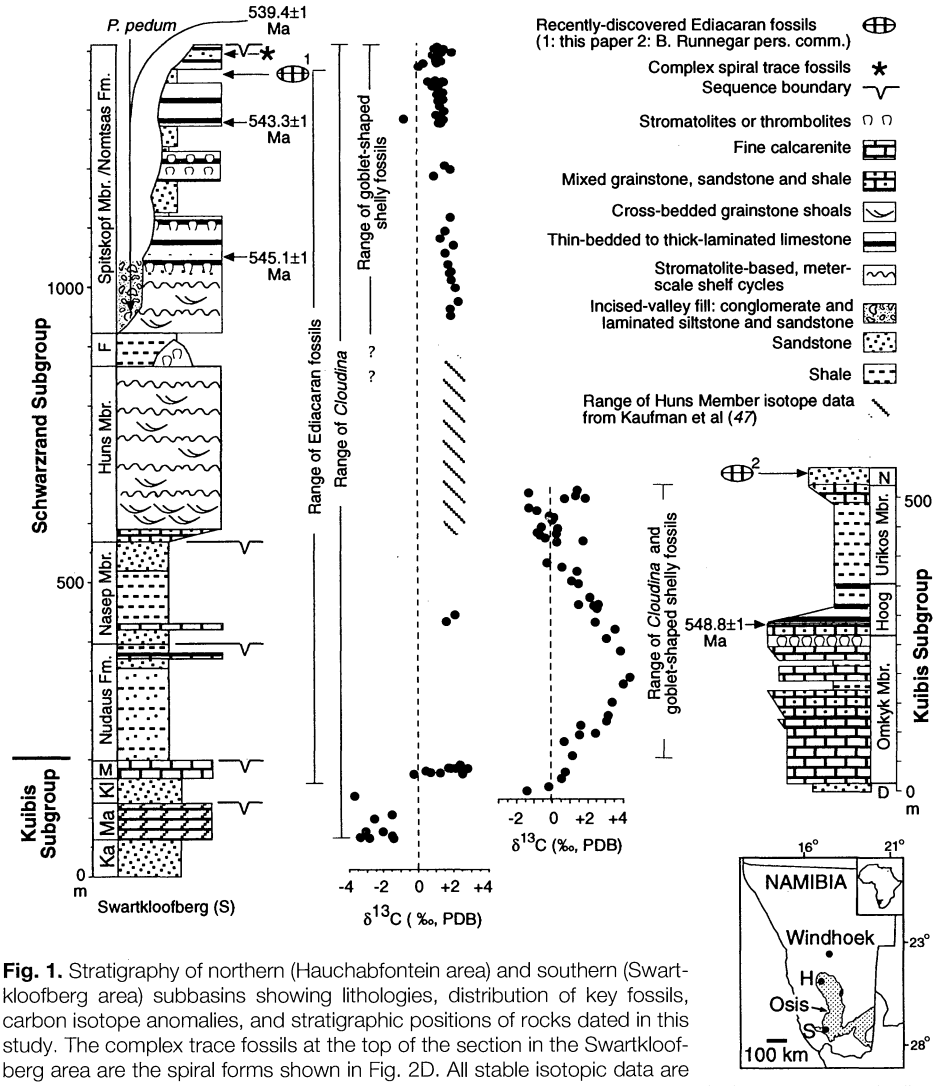

Fig. 1. Stratigraphy of northern (Hauchabfontein area) and southern (Swartkloofberg area) subbasins showing lithologies, distribution of key fossils, carbon isotope anomalies, and stratigraphic positions of rocks dated in this study. The complex trace fossils at the top of the section in the Swartkloofberg area are the spiral forms shown in Fig. 2D. All stable isotopic data are from (*50*) with the exception of the diagonally hachured band, which are from (*47*). Inset shows distribution of Nama Group outcrop (gray) and locations of Hauchabfontein and Swartkloofberg areas in southern Namibia. Ka, Kanies Member; Ma, Mara Member; Kl, Kliphoek Member; M, Mooifontein Member; F, Feldschuhhorn Member; D, Dabis Formation; Hoog, Hoogland Member; N, Niederhagen Member (Schwarzrand Subgroup); and H, Hauchabfontein.

mate; the Slawatycze Formation is known exclusively from subsurface drill-hole data and is thought to correlate lithologically with the volcanogenic Volhyn Group in the Ukraine, which, in turn, is overlain by the Ediacaran-fossil bearing Redkino interval (*30, 31*).

The Precambrian-Cambrian boundary is defined as the point in rock at a section located in southeastern Newfoundland where the trace fossil *Phycodes pedum* first appears (*32*). However, no volcanic rocks are present at or in close proximity to the boundary (*32, 33*). Consequently, the age of the boundary can be calibrated only through correlation with other reference sections that do contain datable volcanic rocks. Over the past decade, estimates of the absolute age of the Precambrian-Cambrian boundary have ranged from 600 to 530 Ma (*13, 34, 35*). Previous U-Pb zircon studies constrain the age of the Precambrian-Cambrian boundary to be younger than about 550 Ma and older than about 544 Ma (*13, 36*).

The best minimum age estimates for the boundary come from ion-microprobe U-Pb studies of volcanic zircons from Lower Cambrian (Tommotian and younger) sections in South Australia, Morocco, and China (*14, 37*) and from conventional zircon studies of volcanic rocks in Siberia and New Brunswick (*13, 38*). Isachsen *et al.* (*38*) reported an age of 531 ± 1 Ma for a volcanic ash just below the Nemakit-Daldyn–Tommotian boundary in New Brunswick. Bowring *et al.* (*13*) obtained an upper intercept age of 543.8 + 5.1/−1.3 Ma (mean $^{207}Pb/^{206}Pb$ age of 543.9 ± 0.2 Ma) for a volcanic breccia intercalated within (*39*) basal Nemakit-Daldyn strata in northeastern Siberia and suggested that the age of the boundary is close to 544 Ma.

The best constraints on the maximum age of the boundary are given by U-Pb zircon ages of 560 ± 1 Ma for the Ercall granophyre of England (*40*), which is unconformably overlain by late Tommotian or early Atdabanian strata, and 551.4 ± 5.8 Ma for a rhyolite flow which lies well below the boundary at Fortune Bay, Newfoundland (*36*).

Previous studies of the age of the Nama Group provide only broad limits. A K-Ar study of detrital white micas from the Nama Group (*41*) led to the conclusion that the upper Nama Group is younger than the youngest detrital white micas (570 Ma) but older than low grade thermal alteration of the upper Nama Group at 530 to 500 Ma.

Vendian to Cambrian Nama Group, Namibia. The Vendian to Cambrian Nama Group is a >3000-m-thick succession of shallow marine and fluvial, siliciclastic and carbonate sedimentary rocks located in southern Namibia (Fig. 1). The Nama Group contains globally recognized Vendian and Cambrian body-fossil, microfossil, and trace-fossil assemblages as well as endemic biotas (*23, 42–46*). Carbonate rocks are abundant throughout most of the Nama Group and their carbon-isotopic variability (*47*) compares well with that from Vendian sections on other continents (*18, 25*). The Nama basin is partitioned into northern and southern subbasins, set apart by the intervening Osis arch, across which most stratigraphic units thin (*48, 49*). We identified and selected several ash beds for dating on the basis of their strategic stratigraphic positions.

Northern subbasin. One ash bed, 94-N-10b, was collected from the Kuibis Subgroup in the northern subbasin (Fig. 1). The Kuibis Subgroup thickens northward from the Osis arch to more than 400 m near Hauchabfontein, where the 30 cm-thick ash bed lies in the Hoogland Member, 270 m above the base of the Kuibis Subgroup. At Hauchabfontein, the Kuibis Subgroup comprises a basal few meters of coarse, transgressive sandstone overlain by shallow marine carbonate platform deposits (*50*) (Fig. 1). Deep-water limestone rhythmite in the Hoogland Member grades upward to shale, which dominates the upper 100 m of the Kuibis Subgroup. The overlying Schwarzrand Subgroup thickens northward from Osis to form a nearly 800 m-thick succession of alternating prodeltaic mudstone and tabular-bedded deltaic sandstone.

Carbon isotope data from the Kuibis Subgroup at Hauchabfontein reveal a positive excursion characterized by $\delta^{13}C$ values that increase upward monotonically from slightly negative at the base to a peak of nearly +5 per mil approximately 60 m below the Hoogland ash; values then decrease to an average of about 0 per mil (*50*) (Fig. 1). Skeletalized fossils occur throughout the Kuibis Subgroup and include *Cloudina* and a previously unreported goblet-shaped form (Fig. 2A). Upward in the section, the Ediacaran fossil *Pteridinium* occurs in the Niederhagen Member of the basal Schwarzrand Subgroup (*51*), and distinctive acritarchs occur in overlying shales (*44*). The carbon isotope pattern and assemblage of fossils are consistent with a Vendian age for at least the Kuibis and lower Schwarzrand subgroups in the northern subbasin.

Southern subbasin. Three volcanic ashes were sampled in the southern subbasin (Fig. 1). The stratigraphically lowest is a 50-cm-

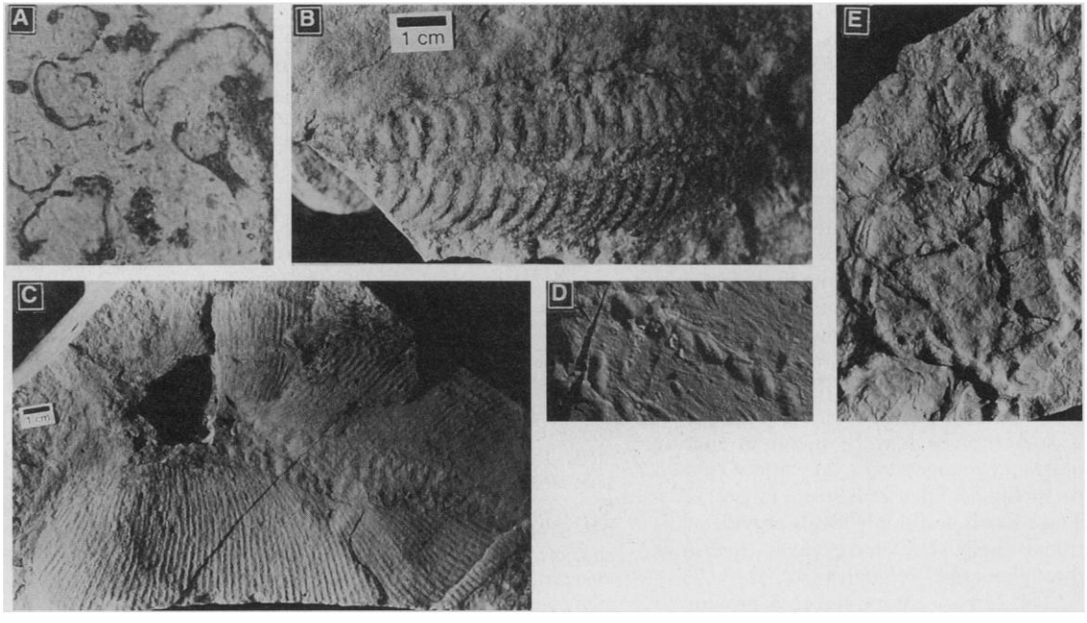

Fig. 2. New fossils from Nama Group. (**A**) Vase-shaped shelly fossils from middle Omkyk Member, Hauchabfontein area. Specimen at right-central part of photograph is approximately 1 cm long. (**B**) *Pteridinium* from upper Spitskopf Member, Swartkloofberg area. (**C**) Possible *Nasepia* or new Dickinsonid-like form from upper Spitskopf Member, Swartkloofberg area. (**D**) Spiral burrow, uppermost Spitskopf Member, Swartkloofberg area. Specimen is approximately 2 cm long. (**E**) *Curvolithus* and *Phycodes pedum* (bottom of photograph) from the incised valley fill of the basal Nomtsas Formation, Sonntagsbrun area. Width of photograph is about 4 cm.

thick bed (sample BZS-7) in the lower part of the Spitskopf Member at Witputs. A second ash (sample 94-N-11), 20 cm thick, is exposed in the uppermost Spitskopf at Swartpunt, 135 m above the lower Spitskopf ash. The third, stratigraphically highest ash (sample 92-N-2) is exposed in the lowermost Nomtsas Formation at Swartkloofberg, a few meters above the sequence boundary that includes the Precambrian-Cambrian boundary.

The Kuibis and Schwarzrand subgroups in the southern subbasin thicken southwestward from the Osis arch to more than 1200 m near Swartkloofberg, where the thickest section is exposed (Fig. 1). The Kuibis Subgroup comprises two depositional sequences, each with basal fluvial to marginal marine sandstone overlain by subtidal carbonate rocks (*49*). Fine-grained, siliciclastic rocks deposited in a shelf and deltaic environment in the lower Schwarzrand Subgroup form two depositional sequences with a combined thickness of more than 350 m (*49*). The upper 600 m of the Schwarzrand Subgroup consists of shallow marine limestone (Huns Member), overlain by siliciclastic mudstone (Feldschuhhorn Member), in turn overlain by mixed deltaic to shallow marine siliciclastic-carbonate rocks (Spitskopf Member). The Spitskopf Member is overlain by the Nomtsas Formation, which forms the highest depositional sequence in the Schwarzrand Subgroup (*49*). The Spitskopf-Nomtsas contact is an erosional surface cut by incised valleys filled with fluvial to shallow-marine conglomerate, sandstone, and shale of the lower Nomtsas Formation (Fig. 1). This surface minimally extends from Swartkloofberg to Sonntagsbrunn, about 100 km to the east (*48*).

$\delta^{13}C$ values are negative in the lower Kuibis Subgroup and increase to values of about +4 per mil in the upper Kuibis Subgroup, similar to the pattern in the northern subbasin (*47*, *50*) (Fig. 1). Above the Kuibis Subgroup, $\delta^{13}C$ values begin near +2 per mil and remain relatively stable through the Huns Member (Kaufman *et al.* 1991) but systematically decrease through the Spitskopf Member to near +1 per mil at its top (*50*). The presence of this trend in the Spitskopf Member is consistent with a latest Vendian age for the top of the Spitskopf Member, as shown by recent work in northern Siberia (*52*). The lack of an overlying negative excursion, however, observed immediately beneath the Precambrian-Cambrian boundary at other localities (*21*, *25*, *52*, *53*), suggests that the youngest Vendian strata in the southern Nama Group either were removed along the sub-Nomtsas erosional surface or never deposited (*50*).

The oldest Ediacaran fossils in the Nama Group (*48*) occur just below the Mooifontein Member of the Kuibis Subgroup, where $\delta^{13}C$ values are high. We found the youngest Ediacaran fossils in the Nama Group near the top of the Spitskopf Member, 90 to 100 m above the upper Spitskopf ash (Fig. 1). Two frond-shaped forms are present (Fig. 2, B and C) including *Pteridinium* and a Dickinsonid-like fossil that may be *Nasepia* or possibly a new taxon (*54*).

The range of skeletalized fossils in the southern subbasin is similar to that of the Ediacaran soft-bodied fossils (Fig. 1). Occurrences of *Cloudina* extend from the lower Kuibis Subgroup through the Spitskopf Member of the Schwarzrand Subgroup (*48*). In addition, the same goblet-shaped skeletalized fossils found in the northern subbasin are also present in the south, extending at least from the top of the Huns Member through the top of the Spitskopf Member. Although previous reports indicate that *Cloudina*-bearing reefs occur in the lower Nomtsas Formation (*48*), it recently has been shown that these reefs actually occur at the top of the underlying Huns Member (*49*).

Simple trace fossils consistent with a Neoproterozoic age are found in the Schwarzrand Subgroup beneath the Nomtsas Formation (*42*, *48*). Complex, spiral trace fossils, possibly of late Vendian age, are seen at the top of the Spitskopf Member (Figs. 1 and 2D). The Cambrian index fossil *Phycodes pedum* was reported from the Nomtsas Formation at Swartkloofberg (*42*) (Fig. 1). We found *Phycodes pedum* in the Nomtsas Formation at Sonntagsbrunn along with the previously unreported Cambrian index fossils *Phycodes coronatum* and *Curvolithus* (Fig. 2E). Poorly preserved specimens of *Tricophycus pedum*, regarded as a Cambrian ichnofossil, recently have been reported from the middle Schwarzrand Subgroup (*55*). If this assignment is correct, then it suggests that this ichnogenera may have a range that extends below the Precambrian-Cambrian boundary, as recognized through chemostratigraphic and biostratigraphic correlations.

In summary, the chemostratigraphy and biostratigraphy of both the southern and northern subbasins of the Nama Group are similar to other Vendian successions around the world. The isotopically enriched carbonates of the Kuibis Subgroup, overlain by the thick Schwarzrand Subgroup containing relatively stable $\delta^{13}C$ values of +1 to +2 per mil, match well with the middle and upper segments of the composite Vendian carbon isotope curve (*18*, *25*). Significantly, many of the world's most diverse assemblages of Ediacaran fossils, including the type assemblage in the Ediacaran Hills of South Australia, occur in rocks deposited during the relatively stable $\delta^{13}C$ interval of +1 to +2 per mil that occurs below the Precambrian-Cambrian boundary (*21*, *25*, *26*). A final, brief negative shift, which occurs at the Precambrian-Cambrian boundary in several sections (*25*), is not present in Namibia, probably because the time that the negative excursion represents is incorporated within the hiatus represented by the Spitskopf-Nomtsas unconformity. Accordingly, the presence of trace fossils of the *Phycodes pedum* zone in strata immediately above the unconformity indicate an earliest Cambrian age for the basal Nomtsas Formation.

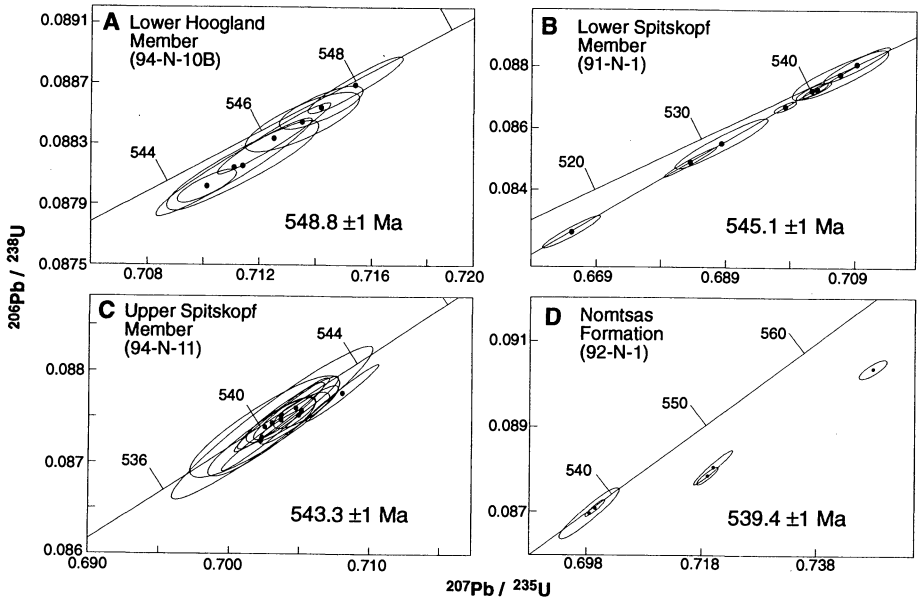

Fig. 3. Concordia diagrams for Nama ash beds dated in this study (**A** through **D**). Ages, in millions of years ago, are marked on the concordia curves. Individual analyses are depicted as 2σ error ellipses. See text for discussion.

U-Pb geochronology of Nama Group

ash beds. We separated zircons using standard techniques from the four samples of volcanic ash collected from the Nama Group. All zircons were air abraded (*56*) prior to dissolution. Both multigrain and single grain analyses (*13, 57*) (Table 1) were performed for the samples, of which two show evidence of an inherited or detrital component.

Sample 94-N-10B [lower Hoogland Member (Fig. 1)] contains abundant clear, doubly terminated zircon crystals. Seven fractions of zircon, including four single grains, yielded a normally discordant ($^{207}Pb/^{206}Pb$ age > $^{207}Pb/^{235}U$ age > $^{206}Pb/^{238}U$ age) cluster of data that do not yield a satisfactory linear regression (Fig. 3A). The age of the sample is best estimated by use of the weighted mean of the $^{207}Pb/^{206}Pb$ ages calculated for all seven fractions. This mean $^{207}Pb/^{206}Pb$ age (95 percent confidence limit) is 548.8 ± 0.3 Ma (MSWD = 0.08) and we adopt an age of 548.8 ± 1 Ma as the best estimate of the age of this ash bed. Because this ash occurs below the base of the late Vendian +2 to +1 per mil carbon-isotopic interval that likely includes many of the world's most diverse assemblages of Ediacaran fossils (*18, 21, 22, 25*), it represents a lower limit for the age of those fossils.

Sample 91-N-1 [lower Spitskopf Member (Fig. 1)] contains abundant, small (50–100 μm), euhedral, zircon grains, many of which are rich in inclusions. The zircons are normally discordant and define a linear array anchored by two concordant analyses (a and b in Table 1). Eight fractions, including four single grains, define a linear array with individual points ranging from 0 to 6.3% discordant. Regression of these eight analyses yields an upper intercept age of 545.6 + 2.5/− 1.9 Ma, a lower intercept of 22.3 ± 83.2 Ma with a MSWD of 0.2 (Fig. 3B). The upper intercept age of 545.6 Ma is interpreted to be the crystallization age of the zircons, but because the lower intercept is essentially 0, the weighted mean of the $^{207}Pb/^{206}Pb$ ages may be a more robust estimate of the crystallization age at 545.1 ± 0.7 Ma (MSWD = 0.22). We suggest that an age 545.1 ± 1 Ma is the best estimate of the age of sample 91-N-1, consistent with its stratigraphically higher position.

Sample 94-N-11 [upper Spitskopf Member (Fig. 1)] contains abundant clear zircons that range from elongate, needle-like zircons (100 to 150 μm in long dimension) to stubby, doubly terminated crystals (50 to 100 μm in long dimension). Fourteen fractions of zircon were analyzed, each containing from 2 to 13 grains (Fig. 3C). Most of the data define a tight cluster around concordia and thus preclude fitting of a regression line to the data. Three analyses (a, b, and c in Table 1) contain a small component of either inherited core material or older detrital grains. The age of the sample is best estimated from the weighted mean of the $^{207}Pb/^{206}Pb$ ages of the remaining 10

Table 1. Uranium-lead isotopic data. Zircon fractions are indicated by letters, and the number of grains is shown in parentheses. Sample weights, estimated using a video monitor with a gridded screen, are known to within 50% error.

Fraction	Weight (μg)	U (ppm)	Pb (ppm)	Total common Pb (pg)	Atomic ratios								Ages		
					$^{206}Pb^*/^{204}Pb$	$^{208}Pb\dagger/^{206}Pb$	$^{206}Pb\dagger/^{238}U$	%err	$^{207}Pb\dagger/^{235}U$	%err	$^{207}Pb\dagger/^{206}Pb$	%err	$^{206}Pb/^{238}U$	$^{207}Pb/^{235}U$	$^{207}Pb/^{206}Pb$
Lower Hoogland Member (94-N-10B)															
a(1)	4	1094.2	102.7	13.6	1668	0.140	0.08854	0.16	0.71419	0.21	0.05850	0.13	546.9	547.2	548.7
b(4)	4	322.0	29.5	3.0	2164	0.144	0.08850	0.45	0.71383	0.47	0.05850	0.10	546.6	547.0	548.7
c(1)	10	287.5	27.6	15.2	1017	0.145	0.08845	0.22	0.71354	0.29	0.05851	0.17	546.3	546.8	549.0
d(1)	5	472.9	43.5	3.9	3262	0.151	0.08829	0.27	0.71216	0.29	0.05850	0.07	545.4	546.0	548.5
e(5)	2	1039.4	99.4	9.4	1068	0.158	0.08816	0.34	0.71142	0.38	0.05853	0.16	544.6	545.6	549.6
f(3)	2	733.0	68.9	6.8	1340	0.154	0.08815	0.37	0.71111	0.39	0.05851	0.11	544.6	545.4	548.9
g(1)	4	1368.0	130.1	8.7	3701	0.185	0.08802	0.12	0.71013	0.15	0.05852	0.08	543.8	544.8	549.1
Lower Spitskopf Member (91-N-1)															
a(5)	3	264.7	25.6	7.5	667	0.158	0.08810	0.68	0.70923	0.73	0.05839	0.25	544.3	544.3	544.3
b(5)	6	98.6	9.6	6.8	530	0.161	0.08778	0.95	0.70675	1.07	0.05839	0.46	542.4	542.8	544.4
c(6)	9	246.3	23.6	11.4	1073	0.172	0.08726	0.28	0.70317	0.30	0.05844	0.11	539.3	540.7	546.4
d(1)	8	250.3	23.7	12.0	909	0.143	0.08723	0.32	0.70239	0.35	0.05840	0.14	539.1	540.2	544.8
e(17)	4	770.1	73.1	10.2	1582	0.183	0.08671	0.22	0.69822	0.26	0.05840	0.14	536.1	537.7	544.8
f(1)	3	195.4	18.0	6.6	531	0.127	0.08552	0.97	0.68845	1.05	0.05839	0.37	529.0	531.9	544.4
g(1)	7	140.9	12.7	3.4	1643	0.178	0.08492	0.59	0.68369	0.61	0.05839	0.12	525.4	529.0	544.6
h(1)	8	130.0	11.6	6.6	797	0.151	0.08261	0.64	0.66516	0.67	0.05840	0.20	511.7	517.8	544.6
Upper Spitskopf Member (94-N-11)															
a(10)	9	247.0	24.3	4.7	2895	0.166	0.09281	0.25	0.78297	0.29	0.06118	0.14	572.1	587.2	645.7
b(13)	6	241.4	24.0	14.6	558	0.164	0.08694	0.45	0.71322	0.75	0.05950	0.57	537.4	546.7	585.4
c(7)	8	188.6	17.4	3.4	2460	0.158	0.08776	0.35	0.70808	0.36	0.05851	0.08	542.3	543.6	549.1
d(12)	12	235.7	21.6	5.5	2942	0.150	0.08757	0.23	0.70520	0.28	0.05841	0.16	541.1	541.9	545.1
e(8)	7	233.5	22.1	5.2	1847	0.183	0.08752	0.37	0.70493	0.40	0.05842	0.14	540.8	541.7	545.5
f(2)	4	243.6	22.2	2.4	2288	0.147	0.08760	0.40	0.70476	0.43	0.05835	0.14	541.3	541.6	543.0
g(5)	5	267.1	25.0	5.0	1518	0.171	0.08754	0.45	0.70386	0.46	0.05832	0.11	540.9	541.1	541.7
h(10)	15	147.6	13.7	9.2	1346	0.139	0.08746	0.29	0.70371	0.36	0.05835	0.20	540.5	541.0	543.1
i(6)	7	171.0	15.6	3.2	2099	0.150	0.08750	0.44	0.70357	0.45	0.05832	0.12	540.7	540.9	541.7
j(6)	13	46.8	4.6	7.2	488	0.174	0.08744	0.97	0.70309	1.02	0.05832	0.29	540.4	540.6	541.7
k(4)	7	129.1	12.2	6.6	806	0.151	0.08739	0.64	0.70254	0.76	0.05831	0.38	540.1	540.3	541.3
l(8)	7	191.3	17.3	3.3	2342	0.141	0.08724	0.38	0.70223	0.39	0.05838	0.08	539.2	540.1	544.1
m(2)	3	271.1	25.1	3.0	1763	0.170	0.08726	0.47	0.70219	0.52	0.05836	0.22	539.3	540.1	543.4
Nomtsas Formation (92-N-1)															
a(18)	18	206.2	20.0	10.3	2015	0.167	0.09035	0.24	0.74780	0.33	0.06003	0.22	557.6	566.9	604.5
b(41)	10	318.9	30.2	8.1	2157	0.169	0.08805	0.46	0.72012	0.47	0.05931	0.12	544.0	550.7	578.7
c(11)	9	278.2	26.4	5.3	2715	0.187	0.08785	0.24	0.71906	0.26	0.05936	0.11	542.8	550.1	580.3
d(18)	18	174.1	16.4	8.4	2060	0.177	0.08708	0.22	0.69946	0.24	0.05826	0.09	538.2	538.5	539.4
e(6)	6	137.0	13.3	8.9	541	0.157	0.08696	0.69	0.69851	0.75	0.05826	0.26	537.5	537.9	539.4

*Measured ratio corrected for fractionation only; Pb fractionation correction is 0.15% ± 0.03% per atomic mass unit. †Corrected for fractionation, spike, blank, and initial common Pb; U blank = 1 pg ± 50%; Pb blank = 3.5 pg ± 50%. Initial common Pb composition is calculated from Stacey and Kramer (*75*) with the interpreted age of the sample. Errors are reported in percent at the two-sigma confidence interval.

fractions. The mean $^{207}Pb/^{206}Pb$ age (95 percent confidence limit) is 543.3 ± 1.0 (MSWD = 0.86). The simplest interpretation of the data is that it is a slightly discordant array, and the best estimate of the age of the ash bed is 543.3 ± 1 Ma. This is interpreted as a maximum age for the Precambrian-Cambrian boundary.

Sample 92-N-1 [basal Nomtsas Formation (Fig. 1)] yielded few zircons that ranged from short stubby clear grains to cloudy inclusion-rich grains. Two single-grain analyses are concordant (d and e in Table 1), one of which has a rather large error ellipse because of a high common Pb content (Fig. 3D). The weighted mean of the $^{207}Pb/^{206}Pb$ ages for these points is 539.4 ± 0.3 Ma. Three additional analyses indicate the presence of a detrital or inherited component and have Pb-Pb ages that range from 577.6 to 603.6 Ma. We interpret 539.4 ± 1 Ma to be the best estimate of the age of this sample and a minimum age for the Precambrian-Cambrian boundary in Namibia.

Age of the Precambrian-Cambrian boundary and duration of Ediacaran animals. The age data of this study yield stratigraphically consistent results for the four ashes distributed over about 1000 m of section in the Nama Group. We have constrained the Precambrian-Cambrian boundary in Namibia to be younger than 543.3 ± 1 Ma and older than 539.4 ± 1 Ma, in good agreement with the upper intercept age of 543.8 + 5.1/−1.3 Ma (weighted mean 207/206 age of 543.9 ± 0.2 Ma) made on the basis of dating the lowermost Cambrian in Siberia (*13*).

A slight contradiction might be implied by the Siberian age of 543.9 Ma, which overlies the terminal Vendian negative $\delta^{13}C$ isotopic excursion, and the Namibian age of 543.3 Ma, which is inferred to underly the same excursion, as we have assumed that the excursion in both localities is related to global seawater composition. However, the analytical uncertainties for the two age determinations overlap, and we take this to indicate that the negative carbon-isotopic excursion lasted 1 million years or less. Furthermore, the surfaces interpreted to include the Precambrian-Cambrian boundary in two important reference sections have approximately the same age, despite strong paleogeographic separation. Whereas the Nama Group was deposited in a foreland basin, isolated near the center of the Gondwanan supercontinent, Siberia wandered independently among a separate collage of continental fragments (*58, 59*).

Our results indicate that the Ediacaran metazoans had a substantial age range with a much younger upper limit than previously thought. Recently, there have been suggestions that some Ediacaran fossils may have a younger upper age limit than was conventionally accepted (*30, 60, 61*). By having calibrated in absolute time an important tie point in the carbon isotope record (*62*) we arrive at the general conclusion that the most diverse Ediacaran fossil assemblages are no more than about 6 million years older than the Precambrian-Cambrian boundary (Fig. 4). Furthermore, the *Pteridinium* and other specimens near the top of the Spitskopf Member provide direct evidence, confirmed by the 543 Ma age for the upper Spitskopf ash, that Ediacaran organisms existed essentially up to at least the time of the Precambrian-Cambrian boundary.

The minimum lower limit for the age range of the Ediacaran fauna is 565 Ma as constrained at Mistaken Point, Newfoundland (*29*). Including this age, we estimate that Ediacaran organisms existed for at least 20 million years. This range may be broadened considerably if the fossils of the Twitya Formation, northwestern Canada, are included. These disk and ring-shaped impressions constitute a low-diversity assemblage of forms that are akin to the simplest representatives from the Ediacaran fauna of the Russian platform (*17, 21*). An approximate age for the Twitya fossils is provided because they underlie Varanger age glaciogenic rocks estimated to have formed close to 600 Ma, as discussed above. Consequently, tissue-grade multicellularity probably evolved at least 35 million years before the oldest dated diverse Ediacaran faunas. Considered collectively, the record of macroscopic animal evolution is interpreted to span a minimum of 55 million years before the Precambrian-Cambrian boundary (Fig. 4).

Implications for early animal evolution. A large gap in the record has been long perceived to exist between the youngest Ediacaran fossils and the oldest diverse invertebrate fossil assemblages near the base of the Cambrian System. However, it now seems likely that the Ediacaran animals existed throughout much of the Vendian (Fig. 4) and that early faunal groups may have experienced greater overlap than previously recognized; the lesson learned from the fossils at the top of the Spitskopf is a reminder that their absence in other contemporaneous strata is more likely an artifact of preservation than an evolutionary obituary. At the same time, a growing number of skeletalized invertebrate fossils can be shown to overlap with the Ediacaran fossils, extending well below the Precambrian-Cambrian boundary. *Cloudina*, once thought to be the only Vendian skeletalized invertebrate, is now joined by the goblet-shaped fossils of the Nama Group. Their ranges completely overlap with the most diverse Ediacaran fossil assemblages (Fig. 4), and they are locally so abundant that they form bioclastic sheets. In addition, through correlation of carbon isotope anomalies, some Cambrian-aspect shelly fossils may now have ranges that extend into the Vendian. *Anabarites* and *Cambrotubulus* appear in uppermost (negative $\delta^{13}C$ values) Vendian strata of Siberia (*53, 63, 64*), and *Anabarites* may be present in somewhat older (positive $\delta^{13}C$ values) strata of Mongolia (*65*).

Once held as the position in the rock record where the major invertebrate groups

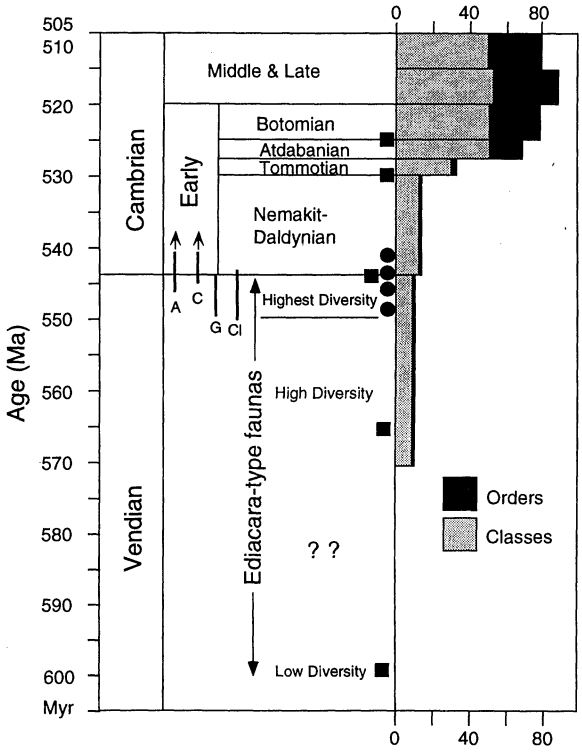

Fig. 4. Revised time scale for the Vendian and Cambrian periods. Key boundaries and events that are constrained by U-Pb zircon chronology are marked by filled circles (this article) or filled squares [other data referenced in the text and in (*13*)]. Diversity data is from Sepkowski (*66*) and diversity divisions for Ediacaran taxa are from Narbonne *et al.* (*21*). Ranges of Vendian age skeletalized fossils are shown: A, *Anabarites*; C, *Cambrotubulus*; Cl, *Cloudina*; and G, goblet-shaped fossils in Nama Group.

first appeared, the Precambrian-Cambrian boundary now serves more as a convenient reference point within an evolutionary continuum. Skeletalized organisms, including Cambrian-aspect shelly fossils, first appear below the boundary (*46*, *64*, *65*) and then show strong diversification during the Early Cambrian (Fig. 4) (*8*, *66*–*68*). Similarly, trace fossils also appear first in the Vendian, exhibit a progression to more complex geometries across the boundary, and then parallel the dramatic radiation displayed by body fossils (*23*, *24*).

Perhaps the Precambrian-Cambrian boundary will acquire new significance in marking the point of extinction of some or all of the Ediacaran organisms given that the impressions at the top of the Spitskopf Member occur just below the boundary. Such a record might be a predictable outcome of extensive predation by more advanced Cambrian organisms (*11*, *69*), although this interpretation conflicts with our evidence that the Ediacaran organisms probably existed concurrently with other major invertebrate groups, including macrophagous predators (*70*). Alternatively, by filling in most of the temporal gap between Ediacaran and Cambrian faunas, the Ediacaran fossils at the top of the Spitskopf Member in Namibia could be used to support evolutionary models that interpret the Ediacaran organisms as ancestors to certain Cambrian metazoans (*9*, *71*–*73*), or as a sister group to the metazoans (*74*). Our data do not force abandonment of any of these hypotheses. Considered collectively, however, the most parsimonious interpretation of the available fossil and age data is that the early development of animals proceeded as a single, protracted evolutionary radiation, culminating in the Cambrian explosion (Fig. 4).

REFERENCES AND NOTES

1. Because of potentially substantial differences in their phylogenetic affinities, we use the term "small shelly fossils/invertebrates" to refer to the distinctive, biomineralized invertebrate fauna of Early Cambrian age, whereas we use the term "skeletalized fossils/invertebrates" more generally to refer to the collective group of Vendian and Early Cambrian biomineralized invertebrate organisms.
2. M. F. Glaessner and M. Wade, *Palaeontology* **9**, 599 (1966).
3. M. A. Glaessner, *The Dawn of Animal Life* (Cambridge Univ. Press, Cambridge, 1984).
4. A. Seilacher, in *Patterns of Change in Earth Evolution*, H. D. Holland and A. F. Trendall, Eds. (Springer-Verlag, Berlin, 1984), pp. 159–168.
5. A. Seilacher, *J. Geol. Soc. London* **149**, 607 (1992).
6. S. J. Gould, *Nat. Hist.* **94**, 22 (1985).
7. _____, *Wonderful Life* (Norton, New York, 1990).
8. J. W. Valentine, in *Origin and Early Evolution of the Metazoa*, J. H. Lipps and P. W. Signor, Eds. (Plenum, New York, 1992).
9. S. Conway Morris, *Palaeontology* **36**, 593 (1993).
10. G. J. Retallack, *Paleobiology* **20**, 523 (1994).
11. A. Seilacher, *Lethaia* **22**, 229 (1989).
12. S. J. Gould, *Sci. Am.* **271**, 84 (1994).
13. S. A. Bowring *et al.*, *Science* **261**, 1293 (1993).
14. W. Compston, I. S. Williams, J. L. Kirschvink, Z. Zichao, M. Guogan, *J. Geol. Soc.* **149**, 171 (1992).
15. R. D. Tucker, T. E. Krogh, R. J. J. Ross, S. H. Williams, *Earth Planet. Sci. Lett.* **100**, 51 (1990).
16. The Vendian System consists of four informal stages including, in ascending order, the Varanger, Volhyn, Redkino, and Kotlin stratigraphic intervals (*19*, *20*).
17. H. J. Hofmann, G. M. Narbonne, J. D. Aitken, *Geology* **18**, 1199 (1990).
18. A. H. Knoll and M. R. Walter, *Nature* **356**, 673 (1992).
19. B. Sokolov and M. A. Fedonkin, *Episodes* **7**, 12 (1984).
20. B. S. Sokolov and A. B. Iwanowski, *The Vendian System—Volume 1* (Springer-Verlag, Berlin, 1990).
21. G. M. Narbonne, A. J. Kaufman, A. H. Knoll, *Geol. Soc. Am. Bull.* **106**, 1281 (1994).
22. R. J. F. Jenkins, *Precambrian Res.* **73**, 51 (1995).
23. G. M. Narbonne, P. M. Myrow, E. Landing, M. M. Anderson, *Can. J. Earth Sci.* **24**, 1277 (1987).
24. T. P. Crimes, in *Origin and Early Evolution of the Metazoa*, J. H. Lipps and P. W. Signor, Eds. (Plenum, New York, 1992), pp. 177–201.
25. A. J. Kaufman and A. H. Knoll, *Precambrian Res.* **73**, 27 (1995).
26. S. D. Pell, D. M. McKirdy, J. Jansyn, R. J. F. Jenkins, *Trans. R. Soc. S. Australia* **117**, 153 (1993).
27. C. A. Kaye and R. F. Zartman, in *Memoir 2: Proceedings "The Caledonides in the USA,"* D. R. Wones, Ed. (Virginia Polytechnic Institute and State University, Blacksburg, VA, 1980), p. 257.
28. T. E. Krogh, D. F. Strong, S. J. O'Brien, V. S. Papezik, *Can. J. Earth Sci.* **25**, 442 (1988).
29. A. P. Benus, in *Trace Fossils, Small Shelly Fossils, and the Precambrian-Cambrian Boundary*, E. Landing, G. M. Narbonne, P. Myrow, Eds. (*Bull. 463*, New York State Museum, Albany, 1988), p. 8.
30. G. Vidal and M. Moczydlowska, *Precambrian Res.* **73**, 197 (1995).
31. B. S. Sokolov and M. A. Fedonkin, *The Vendian System* (Springer-Verlag, Heidelberg, Germany, 1990), vol. 2.
32. E. Landing, in *Origin and Early Evolution of the Metazoa*, J. Lipps and P. Signor, Eds. (Plenum, New York, 1992), pp. 283–309.
33. P. M. Myrow and R. N. Hiscott, *Paleogeogr. Paleoclimatol. Paleoecol.* **104**, 13 (1993).
34. J. W. Cowie and W. B. Harland, in *The Precambrian-Cambrian Boundary*, J. W. Cowie and M. D. Brasier, Eds. (Clarendon, Oxford, 1989), p. 186.
35. G. S. Odin *et al.*, *Nature* **301**, 21 (1983).
36. R. D. Tucker and W. S. McKerrow, *Can J. Earth Sci.* (in press).
37. J. A. Cooper, R. J. F. Jenkins, W. Compston, I. S. Williams, *J. Geol. Soc.* **149**, 185 (1992).
38. C. E. Isachsen, S. A. Bowring, E. Landing, S. D. Samson, *Geology* **22**, 496 (1994).
39. This breccia occurs at the same stratigraphic position, in numerous sections along the Khorbusounka River (*53*).
40. R. D. Tucker and T. C. Pharaoh, *J. Geol. Soc.* **148**, 435 (1991).
41. U. E. Horstmann, H. Ahrendt, N. Clauer, H. Porada, *Precambrian Res.* **48**, 41 (1990).
42. G. J. B. Germs, *J. Paleontol.* **46**, 864 (1972).
43. _____, *Am. J. Sci.* **272**, 752 (1972).
44. _____, A. H. Knoll, G. Vidal, *Precambrian Res.* **32**, 45 (1986).
45. P. T. Crimes and G. J. B. Germs, *J. Paleontol.* **56**, 890 (1982).
46. S. W. F. Grant, *Am. J. Sci.* **290-A**, 261 (1990).
47. A. J. Kaufman, J. M. Hayes, A. H. Knoll, G. J. B. Germs, *Precambrian Res.* **49**, 301 (1991).
48. G. J. B. Germs, in *Evolution of the Damara Orogen*, R. M. Miller, Eds. (*Spec. Publ. 11*, Geological Society of South Africa, 1983), pp. 89–114.
49. B. Z. Saylor, J. P. Grotzinger, G. J. B. Germs, *Precambrian Res.* **73**, 153 (1995).
50. B. Z. Saylor, J. P. Grotzinger, A. J. Kaufman, F. Urban, in preparation.
51. B. Runnegar, personal communication.
52. S. M. Pelechaty, A. J. Kaufman, J. P. Grotzinger, *Geol. Soc. Am. Bull.*, in press.
53. A. H. Knoll, J. P. Grotzinger, A. J. Kaufman, P. Kolosov, *Precambrian Res.* **73**, 251 (1995).
54. The samples have been forwarded to G. Narbonne, Queens University, for taxonomic study. The stratigraphic position of these fossils extends the range of Ediacaran-type fossils in the Nama Group 600 m upward from the highest previous reports in the Huns Member and constrains the range of *Pteridinium* in the Nama Group to be greater than 1000 m.
55. G. Geyer and A. Uchman, *Beringeria Spec. Issue 2*, p. 175 (1995).
56. T. E. Krogh, *Geochim. Cosmochim. Acta* **45**, 637 (1982).
57. C. E. Isachsen, S. A. Bowring, E. Landing, S. D. Samson, *Geology* **22**, 496 (1994).
58. J. L. Kirschvink, in *The Proterozoic Biosphere*, J. W. Schopf and C. Klein, Eds. (Cambridge University Press, Cambridge, 1992), pp. 569–581.
59. P. F. Hoffman, *Science* **252**, 1409 (1991).
60. R. J. Horodyski, J. G. Gehling, S. Jensen, B. Runnegar, *Geol. Soc. Am. Cord. Sect. Abstr. Programs* **26**, A60 (1994).
61. W. Compston *et al.*, *J. Geol. Soc. London* **152**, 599 (1995).
62. A corollary of this age determination is that the late Vendian carbon isotopic interval of +2 to +1 had a duration of about 5 million years, in contrast to previous estimates of about 30 million years (*18*) and about 15 million years (*25*).
63. G. A. Karlova, *Nauka* (Moscow) **292**, 204 (1987).
64. V. V. Khomentovsky and G. A. Karlova, *Geol. Mag.* **130**, 29 (1993).
65. M. Brasier, personal communication.
66. J. J. Sepkoski, in *The Proterozoic Biosphere*, J. W. Schopf and C. Klein, Eds. (Cambridge University Press, Cambridge, 1992), pp. 553–561.
67. J. W. Valentine, S. M. Awramik, P. W. Signor, P. M. Sadler, *Evol. Biol.* **25**, 279 (1991).
68. A. H. Knoll, A. J. Kaufman, M. A. Semikhatov, J. P. Grotzinger, W. Adams, *Geology* (in press). The data in this paper suggest that many "Tommotian" taxa thought to mark the base of that stage may have evolved sequentially throughout the Nemakit-Daldyn Stage.
69. M. A. S. McMenamin and D. L. S. McMenamin, *The Emergence of Animals—The Cambrian Breakthrough* (Columbia Univ. Press, New York, 1990).
70. S. Bengtson and Y. Zhao, *Science* **257**, 367 (1992).
71. M. A. Fedonkin, *White Sea Biota of the Vendian: Precambrian Nonskeletal Fauna of the Northern Russian Platform* (in Russian) (Trudy Akademiya Nauk SSR, vol. 342, 1981).
72. R. J. F. Jenkins, in *Origin and Early Evolution of the Metazoa*, J. H. Lipps and P. W. Signor, Eds. (Plenum, New York, 1992), pp. 131–176.
73. B. Runnegar, in *Early Life on Earth*, S. Bengtson, Ed. (Columbia Univ. Press, New York, 1994), pp. 287–297.
74. L. W. Buss and A. Seilacher, *Paleobiology* **20**, 1 (1994).
75. J. S. Stacey and J. D. Kramer, *Earth Planet. Sci. Lett.* **26**, 207 (1975).

76. We thank G. Germs, S. Jensen, A. Knoll, P. Myrow, G. Narbonne, and B. Runnegar for sharing data and helpful discussions, and the Geological Survey of Namibia, NSF, and NASA for support. A. Knoll, G. Narbonne and B. Runnegar provided expertise in fossil identification. C. Isachsen and D. Hawkins refined low-blank geochemistry at MIT, and K. Davidek helped in zircon separation and selection; B. Smith, F. Urban, A. Khelani, and M. Coyne provided field assistance. D. Erwin, G. Geyer, A. Knoll, B. Runnegar, D. Winston and two anonymous reviewers suggested helpful revisions to the text.

26 July 1995; accepted 28 September 1995